Bulk **A**coustic **R**esonator FEM-BEM Simulation

INTRODUCTION

In RF communication systems, **B**ulk **A**coustic **W**ave (BAW) filters can offer superior performance and reduced size and cost compared to SAW and ceramic filters. The purity of the resonance and the quality factor *Q* of BAW resonator are key parameters in order to reach filter specifications. In a **S**olidly **M**ounted **R**esonator (SMR), the thickness resonator (thin piezoelectric layer between two electrodes) is deposited on a multi-layered Bragg reflector that is designed to decouple resonator from substrate (Fig. 1). In a **F**ilm **B**ulk **A**coustic **R**esonator (FBAR), the thickness resonator (thin piezoelectric membrane between two electrodes) is also deposited on a multi-layered Bragg reflector that is designed to decouple resonator from substrate (Fig. 2). Thus, in both cases, the coupling between resonator and substrate has a major influence on the quality factor (elasto-dynamic radiation in the substrate) and spurious modes (resonances of laterally propagating pseudo-Rayleigh waves) and must be accurately modeled.

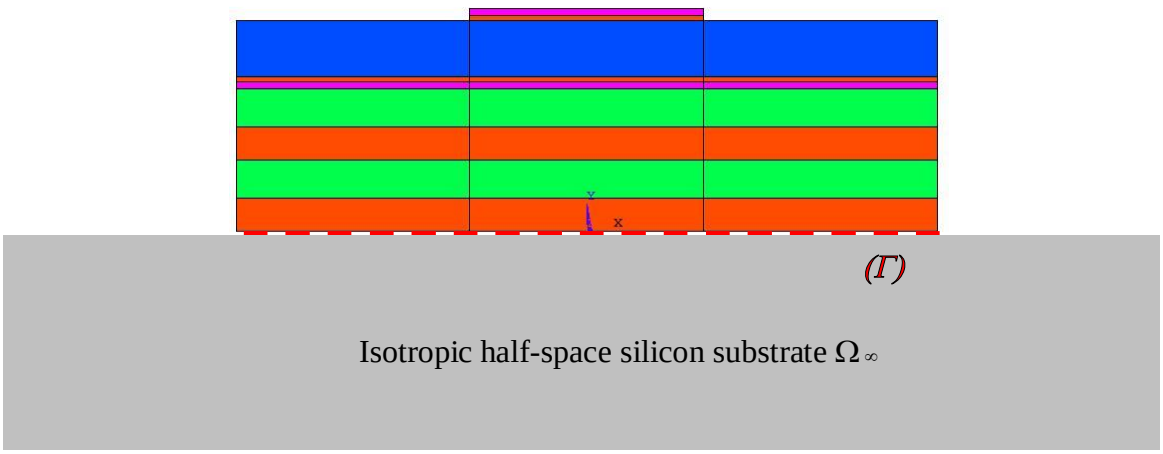

Figure 1. Geometry of a SMR

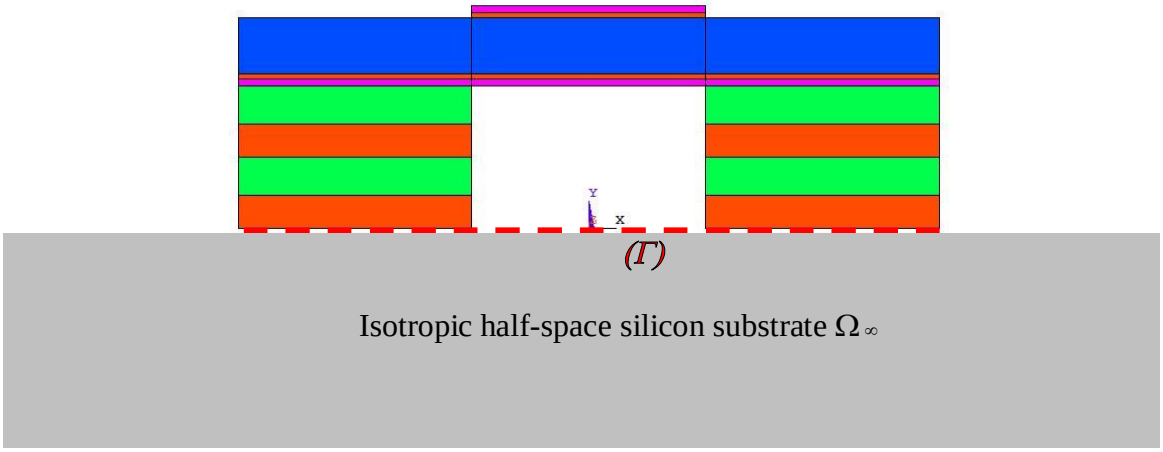

Figure 2. Geometry of a FBAR

NUMERICAL MODEL

The resonator and the Bragg reflector constitute a close solid domain Ω_s containing a piezoelectric sub-domain Ω_p (blue layer) (Fig. 1) and (Fig. 2). This domain is in contact with an infinite homogeneous isotropic elastic half-space Ω_∞ by surface (Γ) pointing towards Ω_∞. All the variables exhibit an implicit $e^{+j\omega\tau}$ dependence where ω denotes the angular frequency and τ the time. In Ω_s, the physical quantities of interest are the displacement vector $\boldsymbol{u}$ and the electric potential ϕ. The nodal values of $\boldsymbol{u}$ and ϕ are the unknowns of the following set of finite element equations [1].

$$\begin{bmatrix} [K]_{\Omega\Omega}-\omega^2[M]_{\Omega\Omega} & [K]_{\Omega\Gamma}-\omega^2[M]_{\Omega\Gamma} & [K_p] \\ \left([K]_{\Omega\Gamma}-\omega^2[M]_{\Omega\Gamma}\right)^T & [K]_{\Gamma\Gamma}-\omega^2[M]_{\Gamma\Gamma} & [0] \\ [K_p]^T & [0] & [K_d] \end{bmatrix} \begin{Bmatrix} \mathbf{U}_\Omega \\ \mathbf{U}_\Gamma \\ \Phi \end{Bmatrix} = \begin{Bmatrix} \mathbf{F}_\Omega \\ \mathbf{F}_\Gamma \\ -\mathbf{Q} \end{Bmatrix} \qquad (1)$$

Where the subscript $_\Omega$ applies to nodes inside Ω_s excluding (Γ), and the subscript $_\Gamma$ applies to nodes on (Γ). $\boldsymbol{\Phi}$ (resp. $\boldsymbol{Q}$) is the vector of the nodal values of the electric potential (resp. electrical charge), $\boldsymbol{U}$ (resp. $\boldsymbol{F}$) is the vector of the nodal values of the displacement (resp. force). $[K]$, $[K_p]$ and $[K_d]$ are respectively the mechanical, piezoelectric and dielectric stiffness matrices. $[M]$ is the consistent mass matrix. As energy is provided by the electrical voltage generator, $\boldsymbol{F}_\Omega = \mathbf{0}$ (no applied external mechanical force) and either $\Phi = \Phi_0$ where Φ_0 is the driving voltage (for each node on the hot electrode) or $\boldsymbol{Q} = \mathbf{0}$ (for the nodes inside Ω_p excluding the hot electrode).

The displacement $\boldsymbol{u}$ on Γ is given by the integral representation [2] and [3].

$$\mathbf{u}(r) = \int_{(\Gamma)} \left[G\left(r - r^{'}\right) \right] \ \mathbf{t}\left(r^{'}\right) \ d\Gamma\left(r^{'}\right) \tag{2}$$

t is the vector of the surface force density applied on *(Γ)*, $r - r^{'}$ the algebraic distance between source and observation points, where *r* and *r'* are positions vectors. [*G*(*r* - *r'*)] is the Green tensor of the isotropic half-space with stress-free surface. It is obtain using the Helmholtz decomposition of elasto-dynamic equation motion in the spatial wave number domain [2] and [3].

For each finite element e of *(Γ)*, the spatial discretization of ***t*** is performed by using the classical FEM interpolation functions [$N^{(e)}$] [4].

$$\mathbf{t}^{e}(r) = \left[N^{e}\left(r\right) \right] \mathbf{T}_{\Gamma}^{e} \tag{3}$$

Where $\boldsymbol{T}_{\Gamma}^{e}$ is the elementary nodal vector of surface force density. Equation (3) is combined with equation (2) for each node on *(Γ)* to lead after assembling to the matrix equation.

$$\mathbf{U}_{\Gamma} = \left[X\left(\omega\right) \right] \mathbf{T}_{\Gamma} \tag{4}$$

With,

$$\left[X\left(\omega\right) \right] = \sum_{e} \int_{(\Gamma^{e})} \left[G\left(r - r'\right) \right] \ \left[N^{e}\left(r'\right) \right] \ d\Gamma^{e}\left(r'\right) \tag{5}$$

In the considered problem, nodal forces $\boldsymbol{F}_{\Gamma}$ appearing in equation (1) are reaction forces of the substrate on Ω_s expressed as [4].

$$\mathbf{F}_{\Gamma} = -\sum_{e} \int_{(\Gamma^{e})} \left[N^{e}\left(r\right) \right]^{T} \mathbf{t}(r) d\Gamma^{e}\left(r\right) = -\left(\sum_{e} \int_{(\Gamma^{e})} \left[N^{e}\left(r\right) \right]^{T} \left[N^{e}\left(r\right) \right] d\Gamma^{e}\left(r\right) \right) \mathbf{T}_{\Gamma} \tag{6}$$

This last equation is combined with equation (5) to get the matrix equation.

$$\mathbf{F}_{\Gamma} = -\left(\sum_{e} \int_{(\Gamma^{e})} \left[N^{e}\left(r\right) \right]^{T} \left[X\left(\omega\right) \right]^{-1} \left[N^{e}\left(r\right) \right] d\Gamma^{e}\left(r\right) \right) \mathbf{U}_{\Gamma} = -\left[Z\left(\omega\right) \right] \mathbf{U}_{\Gamma} \tag{7}$$

Where [$Z(\omega)$] is an impedance matrix. It is a frequency dependent, complex, non-symmetric and fully populated matrix. Thus, the final set of equations is obtained by combining equations (1) and (7).

$$\begin{bmatrix} [K]_{\Omega\Omega} - \omega^2[M]_{\Omega\Omega} & [K]_{\Omega\Gamma} - \omega^2[M]_{\Omega\Gamma} & [K_p] \\ \left([K]_{\Omega\Gamma} - \omega^2[M]_{\Omega\Gamma}\right)^T & [K]_{\Gamma\Gamma} - \omega^2[M]_{\Gamma\Gamma} + \left[Z(\omega)\right] & [0] \\ [K_p]^T & [0] & [K_d] \end{bmatrix} \begin{Bmatrix} \mathbf{U}_\Omega \\ \mathbf{U}_\Gamma \\ \Phi \end{Bmatrix} = \begin{Bmatrix} 0 \\ 0 \\ -\mathbf{Q} \end{Bmatrix} \qquad (8)$$

RESULTS

Two-dimensional and three-dimensional simulations are conducted for an aluminium nitride (AlN) piezoelectric resonator with molybdenum (Mo) electrodes isolated from silicon substrate by a four-layer Bragg reflector made of tungsten-silicon oxide (W/SiO_2) stacks. Layer thicknesses of Bragg reflector are all set to $\lambda/4$ where λ is the wavelength of the longitudinal wave. Layer widths are 50 μm for the top electrode and 75 μm for the other layers. Material losses are not included in the model.

Resonator impedances (modulus and phase) computed with 1D, 2D and 3D FEM-BEM and compared. Main differences between simulations and associated physical mechanisms are discussed hereafter:

i) 2D and 3D results display spurious peaks which are related to the lateral resonances of the pseudo-Rayleigh waves [5]. Only pseudo-Rayleigh waves which are not (or are weakly) radiating into the substrate during their propagation can build-up the resonance and appear as spurious peak in impedance curves.

ii) Effective coupling coefficients k^2 are computed according to the formula:

$$k^2 = \frac{\pi}{2}\frac{f_s}{f_p}\tan\left(\frac{\pi}{2}\left(\frac{f_p - f_s}{f_p}\right)\right) \qquad (9)$$

Where f_s and f_p are the series (maximum of admittance modulus) and parallel (minimum of admittance modulus) resonance frequencies respectively. Lower coupling coefficients are obtained in the case of the 3D model (Table 1 and Table 2). This slight decrease results from the vibrational energy stored in the lateral waves.

iii) Quality factors are lower in the 2D and 3D simulation (Table 1 and Table 2) due to the additional radiation into the substrate of the lateral pseudo-Rayleigh waves. As internal losses are not included in the model, 2D computed values remain higher than commonly measured values, while 3D computed values are near to commonly measured values. It can also be noted that the computed quality factor is lower at parallel resonance (Q_p) than at series resonance (Q_s). This last result is in good agreement with a previous analysis of the energy loss mechanisms in SMR [6].

RESULTS FOR THE SMR

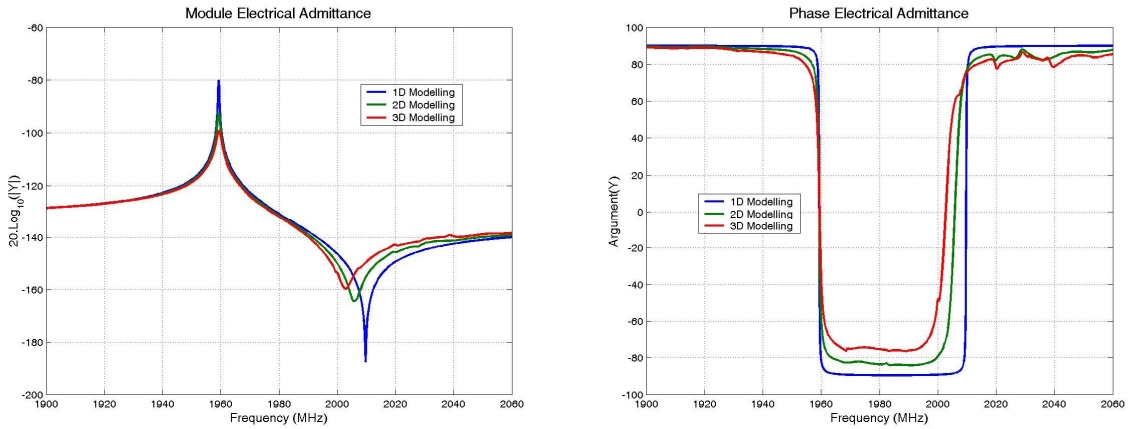

Figure 3. Resonator impedance modulus and phase versus frequency.

Table 1. Computed quality factors and effective coupling coefficients

	f_s	f_p	k^2	Q_s @-3dB	Q_p @-3dB
1D	1959.27 MHz	2009.74 MHz	6.04 %	9752	9484
2D	1959.31 MHz	2005.81 MHz	5.59 %	2730	633
3D	1959.36 MHz	2002.30 MHz	5.18 %	1447	570

RESULTS FOR THE FBAR

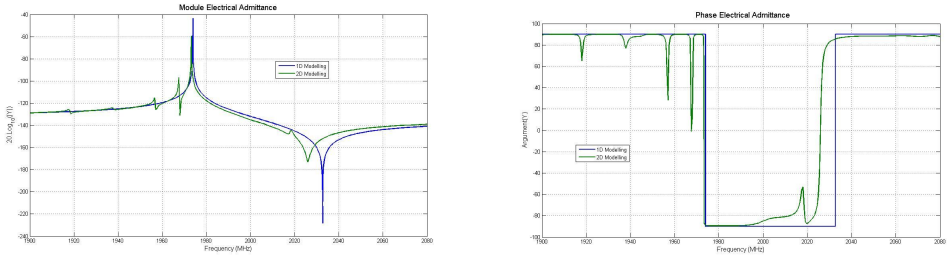

Figure 4. Resonator impedance modulus and phase versus frequency.

Table 2. Computed quality factors and effective coupling coefficients

	f_s	f_p	k^2	Q_s @-3dB	Q_p @-3dB
1D	1973.87 MHz	2032.64 MHz	6.93 %		
2D	1973.15 MHz	2025.97 MHz	6.27 %	19731.50	1873.47

CONCLUSION

To simulate Solidly Mounted Resonators, two-dimensional and three-dimensional numerical models, based on the FEM representation of the resonator and the Bragg reflector and the BEM description of the substrate, have been developed. Elastodynamic energy radiation into the substrate is included in the model and thus SMR and FBAR quality factors are evaluated. Numerical results are presented for an aluminium nitride resonator with molybdenum electrodes operating at 1.96 GHz and decoupled from the substrate by a tungsten-silicon dioxide de Bragg reflector.

ACKNOWLEDGEMENTS

This work was done in collaboration with IEMN- UMR CNRS 8520 and STMicroelectronics.

REFERENCES

[1] H. Allik, T. J. R. Hughes, “Finite element method for piezoelectric vibration”, Int. J. Numer. Methods Eng. Vol. 2, 151-157, (1970).

[2] I.A. Viktorov, "Rayleigh and Lamb waves", Plenum Press New York, (1967).

[3] G.F Miller and H. Pursey, ’’The field and radiation impedance of mechanical radiators on the free surface of a semi-infinite isotropic solid’’. Proc R. Soc. Vol. 223, pp. 521-541, (1954).

[4] O.C. Zienkiewicz and R.L. Taylor, "The Finite Element Method", 4th ed., McGraw-Hill New Yokk, (1989).

[5] G.C. Faittinger, S. Marksteiner, J. K. Kaitila and R. Aigner, "Optimization of acoustic dispersion for high performance thin film BAW resonators", 2005 IEEE Ultrasonics Symposium, pp 1175-1178.

[6] R. Thalhammer and R. Aigner, "Energy loss mechanisms in SMR-type BAW devices", 2005 IEEE MTT-S Microwave Symposium.